

Supplementary Information for

**Impact of Intrinsic Framework Flexibility for Selective Adsorption of Sarin in
Non-Aqueous Solvents using Metal-Organic Frameworks**

Jongwoo Park¹, Mayank Agrawal¹,
Dorina F. Sava Gallis², Jacob A. Harvey³, Jeffery A. Greathouse³, and David S. Sholl^{1*}

¹ School of Chemical & Biomolecular Engineering, Georgia Institute of Technology, Atlanta, GA 30332 USA

² Nanoscale Sciences Department, Sandia National Laboratories, Albuquerque, NM 87185 USA

³ Geochemistry Department, Sandia National Laboratories, Albuquerque, NM 87185 USA

* Corresponding author. E-mail: david.sholl@chbe.gatech.edu.

Table of Contents

S1. MOF Material Set

S2. Adsorption Conditions for Solvents and Mixtures

S3. Adsorption Selectivity in Rigid and Intrinsically Flexible MOFs

S4. Effect of MOF Properties on Quantitative Predictions of Adsorption Selectivity

S5. Molecular Modeling Details

S6. Numerical Data for Analysis

References

S1. MOF Material Set

Table S1 curates a list of 23 MOFs chosen via MOF selection criteria illustrated in Fig. 1 in the main text.

Table S1. List of 23 MOFs chosen via MOF selection criteria. MOFs are listed with CSD reference codes reported in the CoRE MOF database¹, except UiO-66-CF₃², in alphabetical order. The physical properties of MOFs are adapted from the CoRE MOF database and calculated for UiO-66-CF₃ in this work.

MOFs	Metal Type	V _P (cm ³ /g)	S _A _{acc} (m ² /g)	LCD (Å)	PLD (Å)
AMAFOK	Cu	0.30	513.32	6.60	5.66
BARZAW	Zn	0.26	337.15	7.74	2.56
BZRZOK	Cu	0.28	340.18	7.66	2.74
COMDOY	Ga	0.48	971.33	6.12	5.54
EGELUY01	Al	0.67	1555.22	7.46	7.05
EHALOP	Al	0.65	1632.09	7.57	7.12
HAFQOW	Al	0.65	1593.41	7.39	6.93
KEDQAN	Zn	0.39	551.92	6.47	4.70
OFORUX	Cd, Cu	0.26	264.75	5.54	5.06
ONIXOZ	Cu	0.74	1971.77	9.94	9.19
OVICUS	Zn	0.29	409.62	5.88	5.25
QONQEQQ	Al	0.67	1519.12	7.41	7.01
RAZYIC	Cu	0.43	1033.43	7.88	6.21
SABVOH	Al	0.59	1333.73	6.27	5.98
SABVOH01	Al	0.59	1377.25	6.49	6.20
SABVUN	Al	0.61	1439.47	7.02	6.76
UiO-66-CF ₃	Zn	0.36	554.21	7.20	3.20
UTEWOG	Ni	0.95	1702.39	14.60	9.55
UTEXAT	Zn	0.61	1068.81	6.27	4.01
UTEXIB	Co	0.60	1082.64	6.30	3.96
WAYMIU	Al	0.60	1412.09	7.35	6.91
WAYMOA	Al	0.65	1471.49	7.08	6.89
XUNJEW	Zn	0.40	778.07	7.72	4.21

* Abbreviations stand for V_P: pore volume; S_A_{acc}: accessible surface area; LCD: largest cavity diameter; and PLD: pore limiting diameter.

S2. Adsorption Conditions for Solvents and Mixtures

Table S2 summarizes Henry constants (K_H) computed via a Widom particle insertion method³ for sarin, soman, and H₂O in 23 MOFs at 298 K as a part of the material selection criteria. K_H calculated for non-aqueous solvents of MeOH and IPA at 298 K are also summarized.

Table S2. Henry constants (K_H) computed for CWAs of sarin, soman, and solvents of H₂O, MeOH, IPA in 23 MOFs at 298 K.

MOFs	$K_{H,\text{sarin}}$	$K_{H,\text{soman}}$	$K_{H,\text{H}_2\text{O}}$	$K_{H,\text{MeOH}}$	$K_{H,\text{IPA}}$
AMAFOK	1.60E-01	1.75E+01	3.90E-06	5.31E-08	1.27E-08
BARZAW	4.47E-01	2.06E-01	1.55E-06	4.43E-08	1.06E-08
BZRZOK	3.75E-01	1.02E-03	2.06E-06	4.61E-08	1.10E-08
COMDOY	6.10E-02	2.52E+02	5.88E-06	6.28E-08	1.50E-08
EGELUY01	6.47E-03	4.73E+01	7.45E-06	1.75E-07	4.18E-08
EHALOP	5.12E-03	5.04E+01	8.36E-06	1.76E-07	4.19E-08
HAFQOW	5.78E-03	4.29E+02	8.11E-06	1.74E-07	4.17E-08
KEDQAN	6.76E-02	8.94E-03	4.41E-06	5.06E-08	1.21E-08
OFORUX	1.48E-01	2.37E-03	2.11E-06	2.68E-08	6.41E-09
ONIXOZ	2.99E-03	1.18E-03	9.09E-06	9.29E-08	2.22E-08
OVICUS	6.34E-01	1.83E-01	8.57E-06	5.59E-08	1.34E-08
QONQEQQ	6.06E-03	2.62E+01	6.88E-06	1.75E-07	4.18E-08
RAZYIC	1.20E-02	5.62E+01	9.39E-06	6.88E-08	1.64E-08
SABVOH	7.91E-02	2.47E+03	6.67E-06	1.65E-07	3.94E-08
SABVOH01	1.14E-01	2.60E+02	6.91E-06	1.64E-07	3.92E-08
SABVUN	2.40E-02	1.53E+02	6.92E-06	1.69E-07	4.03E-08
UiO-66-CF ₃	9.49E-03	1.20E-02	2.03E-06	3.74E-07	1.90E-07
UTEWOG	4.21E-02	7.69E+00	8.90E-06	1.05E-07	2.52E-08
UTEXAT	4.98E-03	1.54E-01	8.36E-06	7.20E-08	1.72E-08
UTEXIB	5.45E-03	5.30E+02	8.32E-06	7.90E-08	1.89E-08
WAYMIU	2.14E-02	2.99E+03	7.62E-06	1.69E-07	4.03E-08
WAYMOA	9.25E-03	9.69E+01	6.29E-06	1.73E-07	4.13E-08
XUNJEW	2.31E-03	3.22E+00	3.53E-06	5.61E-08	1.34E-08

For the bulk mixture adsorption condition, the partial pressure of each solvent was set to represent MOFs being exposed to liquid solvents. It is useful to understand whether the pores of the MOFs would be filled by solvent molecules under these conditions. We examined this by performing single component GCMC simulations of each solvent in the rigid MOF structure. Fig. S1 shows the resulting adsorption loading from GCMC at P^0_{solvent} as well as a simple approximate of the saturation loading of each solvent ($N_{\text{sat},\text{approx}}$) as calculated with Eq. (S1) using the room temperature liquid density of each solvent ($\rho_{\text{liq,solvent}}$)⁴. It is clear that under these conditions the pore of each MOF are essentially completely filled with solvent molecules.

$$N_{\text{sat},\text{approx}} \approx V_P \cdot \rho_{\text{liq,solvent}} \cdot \frac{1}{\text{MW}_{\text{solvent}}} \quad (\text{S1})$$

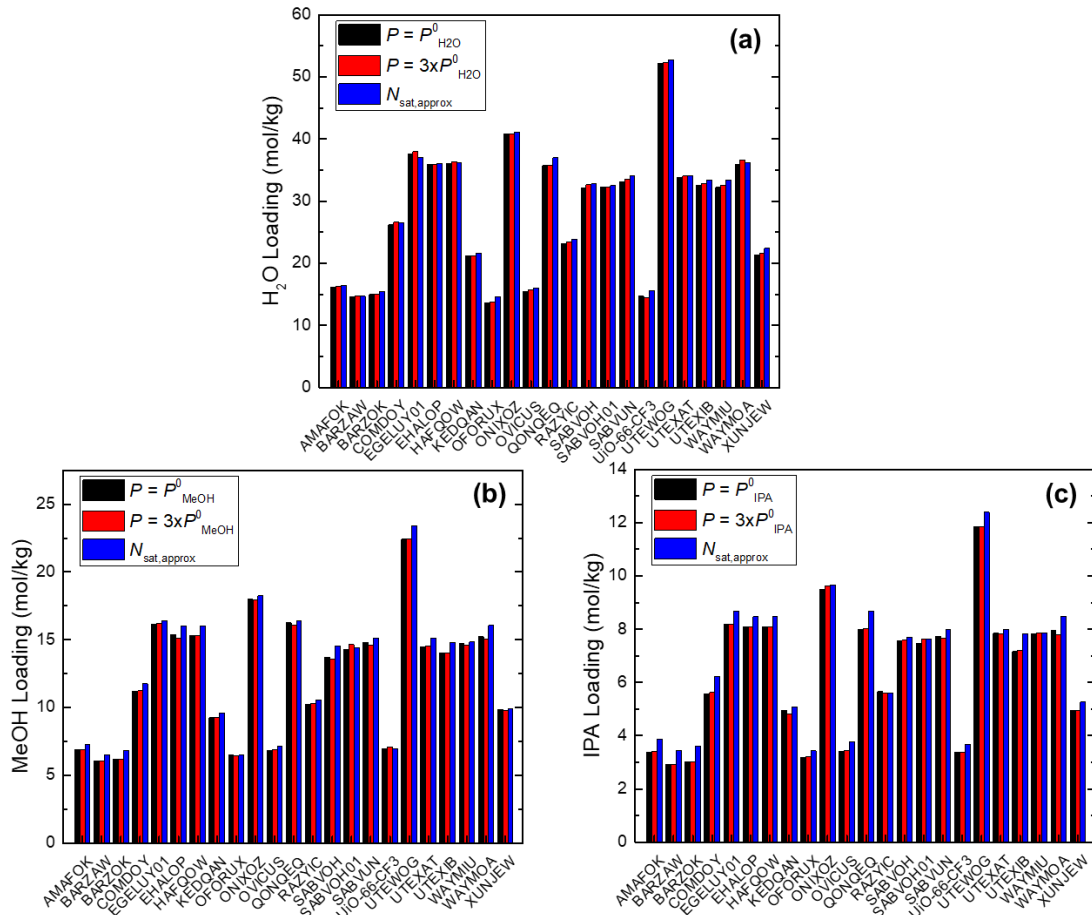


Fig. S1. Comparison of solvent loadings estimated via single component GCMC simulations at $P = P^0_{\text{solvent}}$ and $3 \cdot P^0_{\text{solvent}}$ ⁵ and $N_{\text{sat},\text{approx}}$ for (a) H_2O , (b) MeOH , and (c) IPA . GCMC at $P = P^0_{\text{solvent}}$ is in good agreement with $N_{\text{sat},\text{approx}}$.

S3. Adsorption Selectivity in Rigid and Intrinsically Flexible MOFs

Fig. S2 shows the loadings of adsorbing molecules and the resulting sarin adsorption selectivity in a representative MOF (CSD reference code BARZAW) for 10 distinct MD snapshots. This material showed the maximum deviation in $S_{\text{Flexible}}/S_{\text{Rigid}}$ for sarin-containing binary mixtures we examined. The variation in the observed properties between different flexible snapshots is small, suggesting that averaging over 10 independent snapshots is adequate to give converged results.

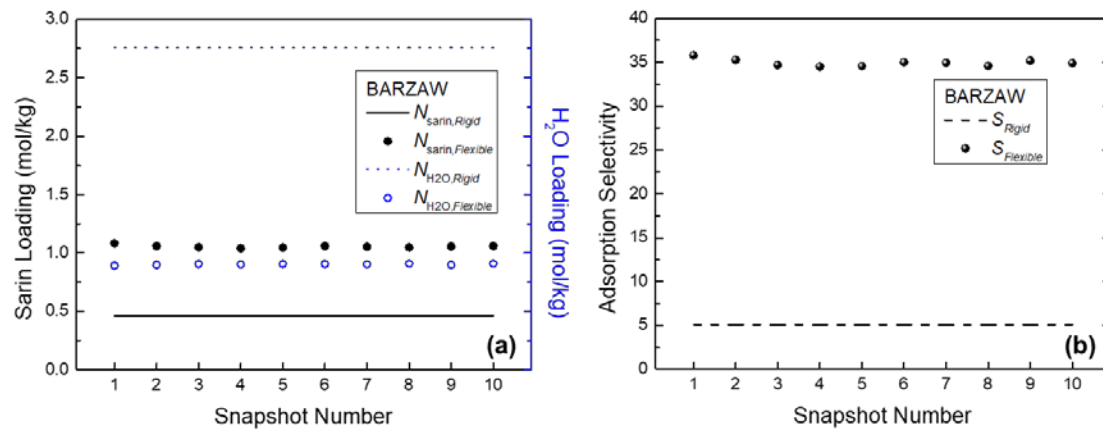


Fig. S2. (a) Adsorption loadings for sarin and H_2O (N_{Flexible}) and (b) adsorption selectivity for sarin (S_{Flexible}) predicted by the flexible snapshot method in different snapshots for a sarin/ H_2O mixture in BARZAW. Adsorption conditions for simulation are as described in the main text. Lines indicate the corresponding adsorption properties predicted by using a rigid structure to guide comparisons.

Fig. S3 shows adsorption selectivity calculations at 298 K at fixed $P/P^0_{\text{sarin}} = 0.25$, and their ratio to allow direct comparisons between two approximations (reproduced from Fig. 3, Fig. 4, and Fig. 5 in the main text). The conclusions of what types of mixture and MOFs could give higher sarin adsorption selectivity, i.e. sarin/ H_2O vs. sarin/MeOH, can be similarly drawn between two approximations, though their numerical deviation is nontrivial.

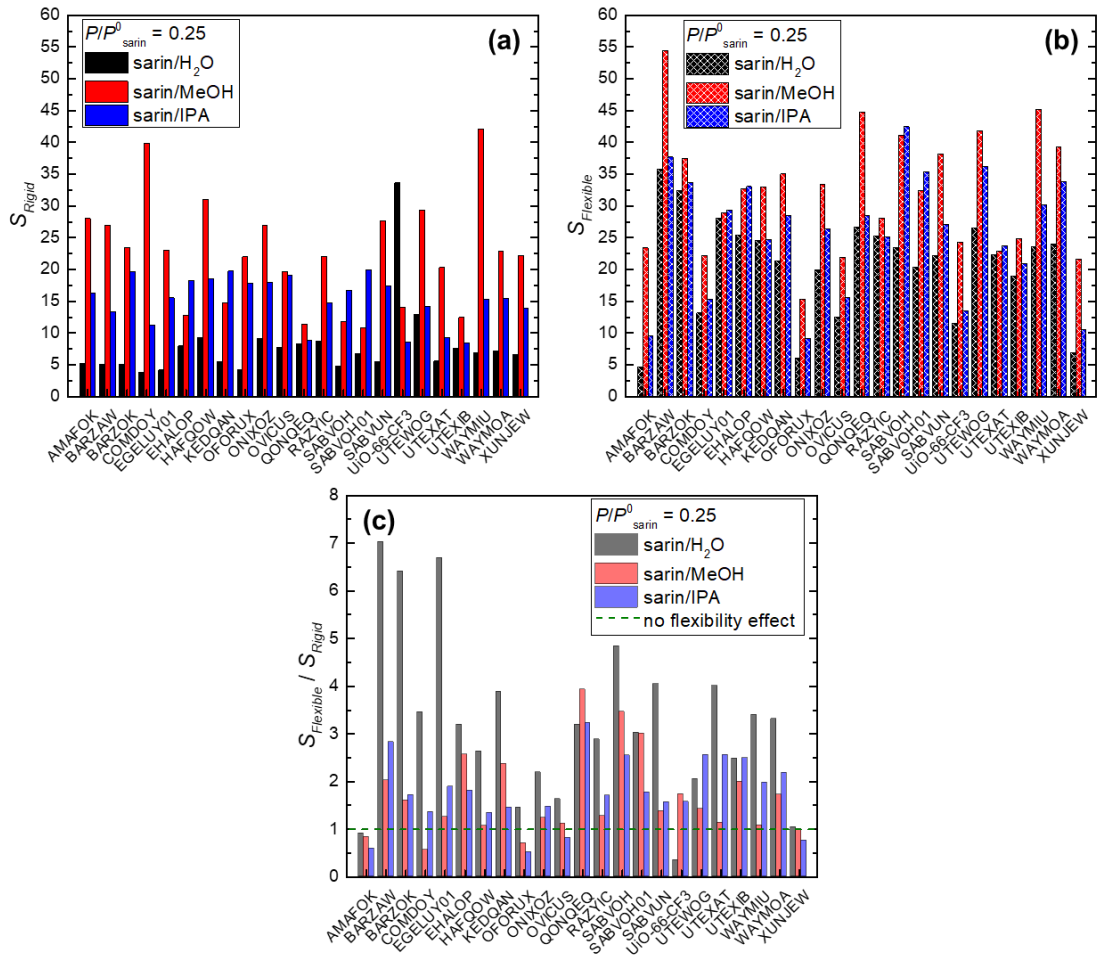


Fig. S3. Adsorption selectivities for sarin at 298 K in 23 MOFs (a) approximated as rigid (S_{Rigid}) and (b) allowed to have intrinsic flexibility ($S_{Flexible}$) for each molecular mixture. (c) Ratio of $S_{Flexible}$ to S_{Rigid} in 23 MOFs for each molecular mixture. A green dashed line shows $S_{Flexible}/S_{Rigid} = 1$ indicating no effect of intrinsic flexibility on adsorption modeling.

Fig. S4a compares the adsorption selectivities for sarin in intrinsically flexible MOFs using realistic polar solvents and the unphysical nonpolar solvents. When solvent molecules were assumed to be nonpolar, the sarin selectivity was substantially decreased in each mixture. Changing from the physical models to unphysical models of solvents made only small differences in the selectivity prediction in rigid MOFs (data not shown). The decreasing trend of adsorption selectivity in the models with nonpolar solvents is associated with a decrease in sarin uptake, $N_{\text{sarin},\text{Flexible}}$, (Fig. S4b) while the uptakes for solvents, $N_{\text{solvents},\text{Flexible}}$, are largely unchanged (inset of Fig. S4b).

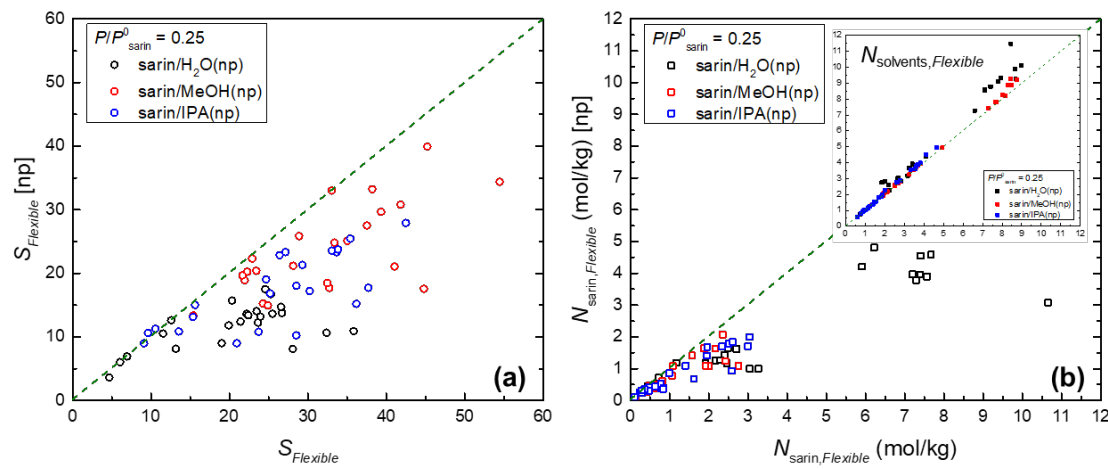


Fig. S4. (a) Parity plot of adsorption selectivity of intrinsically flexible MOFs using polar solvents (horizontal axis) and nonpolar solvents (vertical axis). (b) Parity plot of adsorption amounts of sarin in intrinsically flexible MOFs using polar solvents (horizontal axis) and nonpolar solvents (vertical axis). The inset figure shows adsorption amounts of solvents with identical axes information.

S4. Effect of MOF Properties on Quantitative Predictions of Adsorption Selectivity

Fig. S5a compares LCD and PLD in rigid MOFs against those in flexible MOFs. Pore sizes in flexible MOFs were averaged over those from each MD snapshot. There were only marginal structural changes in MOFs by including intrinsic flexibility ($\Delta V = 0$).

Fig. S5b and Fig. S5c show the ratio of adsorption selectivity in rigid and flexible MOFs as a function of LCD of each MOF using polar and nonpolar solvent molecules, respectively. MOFs that have small LCDs are more affected by intrinsic flexibility. However, we find insufficient correlation considering LCDs to identify the underlying reasons for the sensitivity of including flexibility as a function of molecular mixtures.

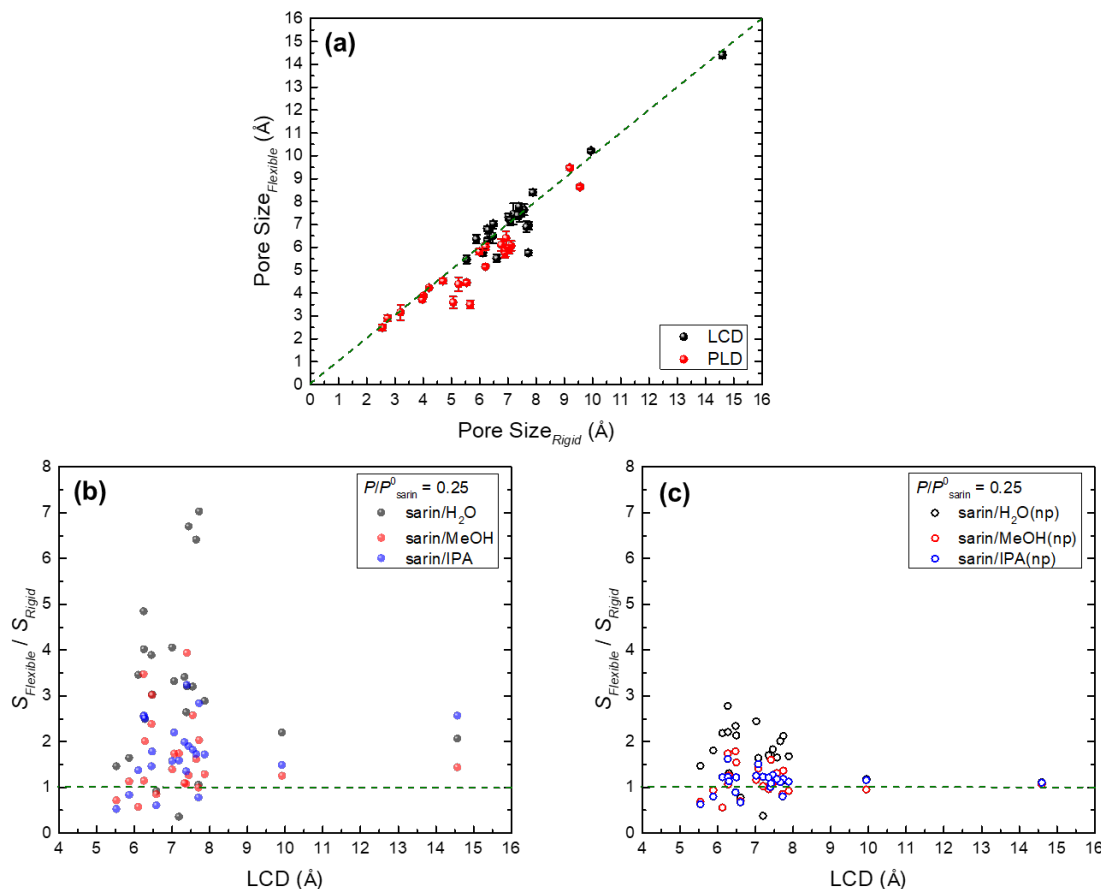


Fig. S5. (a) Parity plot of pore sizes, i.e. LCD and PLD, of 23 MOFs calculated in rigid approximation (horizontal axis) and in intrinsically flexible approximation (vertical axis). Error bars for Pore Size_{Flexible} show variation over ten distinct MD snapshots. $S_{Flexible}/S_{Rigid}$ as a function of LCD with simulations of using (b) realistic polar solvents and (c) unphysical nonpolar (np) solvents. LCD in (b) and (c) are that for rigid MOFs.

S5. Molecular Modeling Details

For GCMC simulations^{6,7}, truncated potentials with tail corrections are applied where Lennard-Jones interactions are truncated at 12 Å. Simulation boxes are expanded to at least 26 Å along *x*, *y*, and *z* dimensions. GCMC simulations included 5,000 initialization cycles followed by 50,000 production cycles for which initial tests indicated good convergence. Henry constants were computed using 200,000 production cycles while including an identical Widom probability.

Pore volumes of computation-ready MOF structures were calculated from the void fractions of each structure using a Widom particle insertion method with a He probe molecule ($\varepsilon/k_B = 10.9$ K, $\sigma = 2.64$ Å) at 298 K.⁷ Accessible surface areas were calculated by using N₂ as probe molecule with overlap distance criteria set to a size parameter σ of 3.31 Å.⁷ Largest cavity diameters and pore limiting diameters were calculated with Zeo++^{8,9} applying the high-accuracy setting with a N₂ probe molecule using a radius of 1.86 Å.⁸

For binary GCMC simulations using “unphysical” nonpolar solvent molecules, we omitted Coulombic adsorbate/adsorbate interactions¹⁰ by removing atomic point charges for solvent molecules. Point charges were retained on sarin in these calculations.

Table S3 summarizes two molecular descriptors for the solvents examined in this work. It shows that molecular mixtures consist of adsorbates of different sizes and polarities.

Table S3. Molecular descriptors for the solvents. Kinetic diameter¹¹ and polarity index^{12,13} of H₂O, MeOH, and IPA are listed. Polarity index is a relative measure of the degree of interaction of the solvent with various polar test solutes.

	H ₂ O	MeOH	IPA
Kinetic diameter, <i>d</i> (Å)	2.6	4.3	4.7
Polarity index	10.2	5.1	3.9

* Sarin¹⁴ has a molecular shape of ~ 5 Å x ~ 12 Å.

S6. Numerical Data for Analysis

Table S4. Numerical data in Fig. 3, Fig. 4, and Fig. 5. Adsorption selectivities for sarin over solvents predicted in rigid MOFs (S_{Rigid}) and intrinsically flexible MOFs ($S_{Flexible}$), and their ratio ($S_{Flexible}/S_{Rigid}$): sarin/H₂O mixture.

MOFs	S_{Rigid}	$S_{Flexible}$	$S_{Flexible}/S_{Rigid}$
AMAFOK	5.16	4.66	0.90
BARZAW	5.10	35.82	7.02
BZRZOK	5.05	32.36	6.40
COMDOY	3.81	13.14	3.45
EGELUY01	4.19	28.07	6.69
EHALOP	7.99	25.46	3.19
HAFQOW	9.36	24.56	2.62
KEDQAN	5.52	21.40	3.88
OFORUX	4.18	6.04	1.44
ONIXOZ	9.10	19.88	2.19
OVICUS	7.72	12.56	1.63
QONQEQQ	8.36	26.69	3.19
RAZYIC	8.80	25.29	2.88
SABVOH	4.85	23.45	4.84
SABVOH01	6.74	20.32	3.03
SABVUN	5.48	22.16	4.04
UiO-66-CF ₃	33.62	11.52	0.34
UTEWOG	12.97	26.57	2.05
UTEXAT	5.59	22.39	4.01
UTEXIB	7.66	18.99	2.48
WAYMIU	6.95	23.62	3.40
WAYMOA	7.23	23.94	3.31
XUNJEW	6.65	6.93	1.04

Table S4. Continued: sarin/MeOH mixture.

MOFs	S_{Rigid}	$S_{Flexible}$	$S_{Flexible}/S_{Rigid}$
AMAFOK	28.06	23.41	0.83
BARZAW	26.99	54.44	2.02
BZRZOK	23.44	37.51	1.60
COMDOY	39.83	22.25	0.56
EGELUY01	23.02	28.86	1.25
EHALOP	12.75	32.71	2.56
HAFQOW	31.04	33.03	1.06
KEDQAN	14.78	35.03	2.37
OFORUX	21.99	15.38	0.70
ONIXOZ	26.99	33.38	1.24
OVICUS	19.67	21.92	1.11
QONQEQQ	11.40	44.77	3.93
RAZYIC	22.09	28.11	1.27
SABVOH	11.86	41.04	3.46
SABVOH01	10.81	32.46	3.00
SABVUN	27.71	38.20	1.38
UiO-66-CF ₃	14.04	24.26	1.73
UTEWOG	29.37	41.82	1.42
UTEXAT	20.30	22.89	1.13
UTEXIB	12.48	24.89	1.99
WAYMIU	42.12	45.23	1.07
WAYMOA	22.83	39.33	1.72
XUNJEW	22.20	21.66	0.98

Table S4. Continued: sarin/IPA mixture.

MOFs	S_{Rigid}	$S_{Flexible}$	$S_{Flexible}/S_{Rigid}$
AMAFOK	16.26	9.61	0.59
BARZAW	13.36	37.70	2.82
BZRZOK	19.70	33.66	1.71
COMDOY	11.32	15.34	1.36
EGELUY01	15.54	29.30	1.89
EHALOP	18.29	33.06	1.81
HAFQOW	18.47	24.67	1.34
KEDQAN	19.74	28.53	1.45
OFORUX	17.83	9.09	0.51
ONIXOZ	17.92	26.38	1.47
OVICUS	19.08	15.60	0.82
QONQEQQ	8.84	28.51	3.23
RAZYIC	14.76	25.17	1.70
SABVOH	16.72	42.49	2.54
SABVOH01	20.01	35.40	1.77
SABVUN	17.42	27.13	1.56
UiO-66-CF ₃	8.61	13.53	1.57
UTEWOG	14.17	36.17	2.55
UTEXAT	9.28	23.70	2.55
UTEXIB	8.39	20.92	2.49
WAYMIU	15.32	30.21	1.97
WAYMOA	15.50	33.84	2.18
XUNJEW	13.87	10.55	0.76

Table S5. Numerical data in Fig. 6 and Fig. 7. Adsorption selectivities for sarin over solvents in rigid MOFs (S_{Rigid}) and intrinsically flexible MOFs ($S_{Flexible}$), and their ratio ($S_{Flexible}/S_{Rigid}$) calculated by using unphysical nonpolar (np) solvents: sarin/H₂O(np) mixture.

MOFs	S_{Rigid}	$S_{Flexible}$	$S_{Flexible}/S_{Rigid}$
AMAFOK	4.64	3.61	0.78
BARZAW	5.13	10.91	2.12
BZRZOK	5.29	10.64	2.01
COMDOY	3.71	8.11	2.19
EGELUY01	4.42	8.10	1.83
EHALOP	8.25	13.64	1.65
HAFQOW	10.74	17.51	1.63
KEDQAN	5.30	12.41	2.34
OFORUX	4.10	6.02	1.47
ONIXOZ	9.98	11.82	1.18
OVICUS	6.97	12.61	1.81
QONQEQQ	8.07	13.74	1.70
RAZYIC	9.95	16.73	1.68
SABVOH	5.05	14.04	2.78
SABVOH01	7.37	15.72	2.13
SABVUN	5.57	13.61	2.45
UiO-66-CF ₃	27.62	10.53	0.38
UTEWOG	13.21	14.72	1.11
UTEXAT	6.06	13.40	2.21
UTEXIB	6.87	8.99	1.31
WAYMIU	7.18	12.25	1.70
WAYMOA	8.04	13.21	1.64
XUNJEW	6.02	6.93	1.15

Table S5. Continued: sarin/MeOH(np) mixture.

MOFs	S_{Rigid}	$S_{Flexible}$	$S_{Flexible}/S_{Rigid}$
AMAFOK	29.11	20.40	0.70
BARZAW	25.20	34.41	1.37
BZRZOK	24.09	27.51	1.14
COMDOY	36.28	20.25	0.56
EGELUY01	23.72	25.86	1.09
EHALOP	13.48	17.71	1.31
HAFQOW	31.70	33.03	1.04
KEDQAN	14.02	25.10	1.79
OFORUX	19.49	13.38	0.69
ONIXOZ	26.02	24.83	0.95
OVICUS	20.17	18.91	0.94
QONQEQQ	10.97	17.58	1.60
RAZYIC	22.90	21.17	0.92
SABVOH	12.08	21.04	1.74
SABVOH01	11.95	18.46	1.55
SABVUN	28.52	33.23	1.16
UiO-66-CF ₃	14.84	15.26	1.03
UTEWOG	28.90	30.80	1.07
UTEXAT	21.03	22.32	1.06
UTEXIB	11.88	14.94	1.26
WAYMIU	41.67	39.92	0.96
WAYMOA	21.08	29.68	1.41
XUNJEW	22.92	19.66	0.86

Table S5. Continued: sarin/IPA(np) mixture.

MOFs	S_{Rigid}	$S_{Flexible}$	$S_{Flexible}/S_{Rigid}$
AMAFOK	15.77	10.62	0.67
BARZAW	14.94	17.72	1.19
BZRZOK	20.92	23.31	1.11
COMDOY	10.73	13.13	1.22
EGELUY01	16.79	21.30	1.27
EHALOP	19.94	23.56	1.18
HAFQOW	18.91	19.05	1.01
KEDQAN	20.17	18.03	0.89
OFORUX	14.26	8.99	0.63
ONIXOZ	19.72	22.84	1.16
OVICUS	18.77	15.02	0.80
QONQEQQ	9.40	10.25	1.09
RAZYIC	14.90	16.82	1.13
SABVOH	17.22	27.92	1.62
SABVOH01	20.86	25.47	1.22
SABVUN	18.56	23.33	1.26
UiO-66-CF ₃	8.80	10.85	1.23
UTEWOG	13.77	15.20	1.10
UTEXAT	8.81	10.79	1.22
UTEXIB	7.93	8.99	1.13
WAYMIU	14.18	17.22	1.21
WAYMOA	15.74	23.76	1.51
XUNJEW	14.05	11.29	0.80

References

- 1 Y. G. Chung, J. S. Camp, M. Haranczyk, B. J. Sikora, W. Bury, V. Krungleviciute, T. Yildirim, O. K. Farha, D. S. Sholl and R. Q. Snurr, *Chem. Mater.*, 2014, **26**, 6185-6192.
- 2 H. Demir, K. S. Walton and D. S. Sholl, *J. Phys. Chem. C*, 2017, **121**, 20396-20406.
- 3 B. Widom, *J. Chem. Phys.*, 1963, **39**, 2808-2812.
- 4 B. S. Furniss, A. J. Hannaford, P. W. G. Smith and A. R. Tatchell, *Practical Organic Chemistry (5th Edition)*, John Wiley & Sons Inc., New York, 1989.
- 5 D. Tang, G. Kupgan, C. M. Colina and D. S. Sholl, *J. Phys. Chem. C*, 2019, **123**, 17884-17893.
- 6 D. Dubbeldam, S. Calero, D. E. Ellis and R. Q. Snurr, *Mol. Simul.*, 2016, **42**, 81-101.
- 7 D. Dubbeldam, A. Torres-Knoop and K. S. Walton, *Mol. Simul.*, 2013, **39**, 1253-1292.
- 8 T. F. Willems, C. H. Rycroft, M. Kazi, J. C. Meza and M. Haranczyk, *Micropor. Mesopor. Mat.*, 2012, **149**, 134-141.
- 9 M. Pinheiro, R. L. Martin, C. H. Rycroft and M. Haranczyk, *CrystEngComm*, 2013, **15**, 7531-7538.
- 10 M. G. Martin and J. I. Siepmann, *J. Phys. Chem. B*, 1998, **102**, 2569-2577.
- 11 M. E. van Leeuwen, *Fluid Phase Equilib.*, 1994, **99**, 1-18.
- 12 D. C. Harris, *Quantitative Chemical Analysis (9th Edition)*, Freeman, New York, 2015.
- 13 E. Katz, R. Eksteen, P. Schoenmakers and N. Miller, *Handbook of HPLC*, Marcel Dekker, New York, 1998.
- 14 R. T. Delfino, T. S. Ribeiro and J. D. Figueroa-Villar, *J. Braz. Chem. Soc.*, 2009, **20**, 407-428.